# Journal Pre-proof

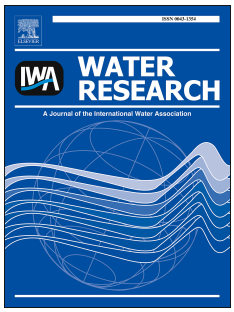


Proxies to monitor the inactivation of viruses by ozone in surface water and wastewater effluent

Camille Wolf, Annalisa Pavese, Urs von Gunten, Tamar Kohn

PII: S0043-1354(19)30862-0

DOI: https://doi.org/10.1016/j.watres.2019.115088

Reference: WR 115088

To appear in: *Water Research*

Received Date: 25 July 2019

Revised Date: 11 September 2019

Accepted Date: 12 September 2019

Please cite this article as: Wolf, C., Pavese, A., von Gunten, U., Kohn, T., Proxies to monitor the inactivation of viruses by ozone in surface water and wastewater effluent, *Water Research* (2019), doi: https://doi.org/10.1016/j.watres.2019.115088.

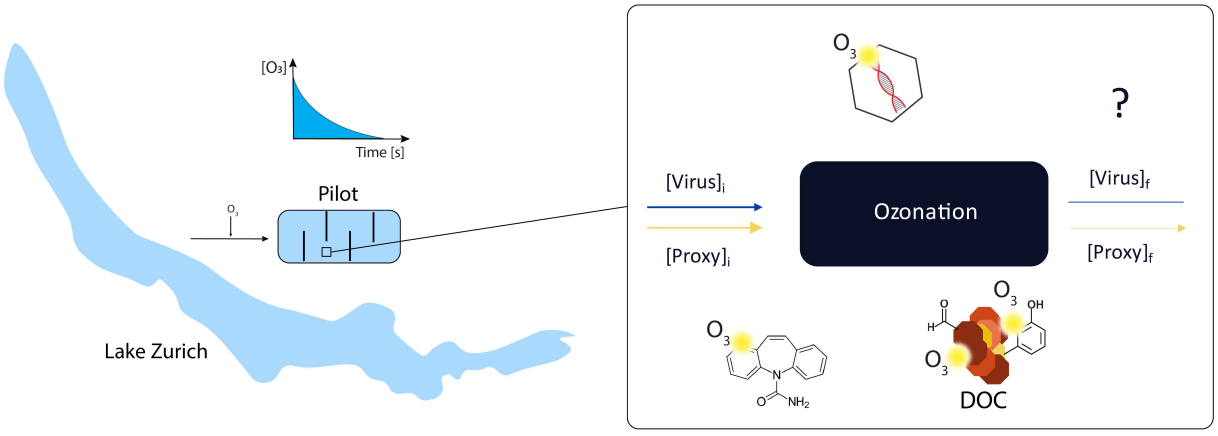

# Proxies to monitor the inactivation of viruses by ozone in surface water and wastewater effluent

Camille Wolf[1], Annalisa Pavese[1], Urs von Gunten[2,3] and Tamar Kohn[1]*

[1] Laboratory of Environmental Chemistry, School of Architecture, Civil and Environmental Engineering (ENAC), École Polytechnique Fédérale de Lausanne (EPFL), CH-1015 Lausanne, Switzerland

[2]Laboratory for Water Quality and Treatment, School of Architecture, Civil and Environmental Engineering (ENAC), École Polytechnique Fédérale de Lausanne (EPFL), CH-1015 Lausanne, Switzerland

[3]Eawag, Swiss Federal Institute of Aquatic Science and Technology, Dübendorf, Switzerland

*Corresponding author email address: tamar.kohn@epfl.ch

Phone: +41 21 693 0891; Fax: +41 21 +41 21 693 80 70

# Abstract

Ozone treatment is an effective barrier against viral pathogens, therefore it is an integral part of many water and wastewater treatment trains. However, the efficacy of ozone treatment remains difficult to monitor, due to the lack of methods to track virus inactivation in real-time. The goal of this work was to identify easy-to-measure proxies to monitor virus inactivation during water and wastewater treatment by ozone. Proxies considered were the abatement in UV absorbance at 254 nm ($UV_{254}$) and carbamazepine (CBZ), a ubiquitous organic micropollutant with a similar abatement rate constant as human viruses. The proxies, as well as the inactivation of two viruses (MS2 coliphage and coxsackievirus B5) were measured in surface water and in a secondary wastewater effluent as a function of the specific ozone dose ($mgO_3$/mg dissolved organic carbon). Virus inactivation was rapid in both matrices, but was more efficient in surface water. This trend was also evident when inactivation was assessed as a function of the ozone exposure to account for the different ozone demand of the two water types. Both proxies, as well as the specific ozone dose, were correlated with virus inactivation. The correlations depended only weakly on the virus species, but – with the exception of CBZ abatement – differed between the two water types. Finally, predictive relationships were established using Bayesian power models, to estimate virus inactivation based on the measurement of a proxy. The models were then applied to estimate the MS2 inactivation in a pilot-scale ozone reactor that treats surface water of Lake Zurich. All proxies yielded good estimates of the actual MS2 inactivation in the pilot plant, indicating that the proxy-inactivation relationships established in the laboratory can also be applied to flow-through reactors. This study confirms that ozone is a highly effective disinfectant for viruses in both surface water and wastewater, and that the abatement of $UV_{254}$ and CBZ can be used to track virus inactivation during water and wastewater treatment.

24 Keywords: ozone; disinfection; coxsackievirus B5; MS2; proxy; wastewater

# 1. Introduction

Human viruses are present in treated sewage at concentrations of $10^4$ to $10^5$ virus particles/L (Farkas et al., 2018; Lodder and de Roda Husman, 2005). If discharged into the environment in an infective state, they can be health risks to recreational water users, or consumers of drinking water, if these waters are used as water resources. The removal and/or inactivation of viruses during water and wastewater treatment is thus an important measure to prevent waterborne diseases. A particularly critical case is potable water reuse, where guidelines aim for 9.5 (Australia) to 12 $\log_{10}$ (California) enteric virus abatement as performance target for a complete treatment train (World Health Organization, 2017).

Ozonation is a promising approach to strongly reduce infective virus concentrations. Ozone is a powerful oxidant that has a long tradition in treatment trains for drinking water (Bicknell and Jain, 2001), and is increasingly implemented for wastewater (Eggen et al., 2014; Ternes et al., 2003; von Gunten, 2018; von Sonntag and von Gunten, 2012) and potable water reuse throughout the world (Gerrity et al., 2013). In a previous study, we determined the inactivation kinetics of a suite of human enteric viruses and bacteriophages by ozone in well-controlled buffered solutions, and second order rate constants for the inactivation of viruses ($k_{O3\text{-}Virus}$) on the order of $10^5$ – $10^6$ $M^{-1}s^{-1}$ were determined (Wolf et al., 2018). However, in natural water or wastewater, the extent of virus inactivation achieved by ozonation remains difficult to predict. First, inactivation kinetics may be mitigated by different matrix constituents (Sigmon et al., 2015), resulting in lower values of $k_{O3\text{-}Virus}$ or in altered inactivation curves. Second, the extent of virus inactivation is a function of the ozone exposure, but this parameter is difficult to measure or estimate in real-time during treatment, due to the high ozone demand of many wastewater or raw drinking water matrices (Buffle et al., 2006b). To overcome this problem, relationships between the ozone exposure and the specific ozone dose ($mgO_3$/mgDOC) have been established (Lee et al., 2014), and can be invoked to estimate the ozone exposure in a given water matrix. However, these

relationships differ between different water matrices and sometimes also on a temporal basis, and are time-consuming and experimentally challenging to establish.

Alternatively, inactivation may be monitored based on an "easy-to-measure" proxy. Proxies are an indirect measure of the ozone exposure, and may be used as surrogate parameters to predict virus inactivation. It has been demonstrated that during ozonation of wastewater, the UV absorbance at 254 nm ($UV_{254}$) of the matrix decreases as a function of the specific ozone dose, which in turn determines the ozone exposure (Bahr et al., 2007; Buffle et al., 2006a). In one study, a correlations between the reduction in $UV_{254}$ and the measured ozone exposure was established (Buffle et al., 2006a), which is the controlling factor for micropollutant abatement as well as the inactivation of the indicator organisms. Based on this approach the abatement of chemical and biological pollutants based can be estimated solely on the measurement of the $UV_{254}$ abatement, without the need to determine the ozone exposure (Buffle et al., 2006a).

In this study, we explored if the abatement of $UV_{254}$ can be used as a proxy for the inactivation of different viruses. Additionally, we investigated if micropollutants with similar ozone reactivity as viruses may serve as alternative proxies. We investigated micropollutants as an additional proxy, because in Switzerland their abatement in wastewater is regularly monitored in the framework of the Swiss water protection act, a new regulation aiming to reduce discharge of micropollutant in the environment (Eggen et al., 2014; OFEV, 2015; Stamm et al., 2015) This is achieved by monitoring a suite of indicator compounds, among them carbamazepine (CBZ), which has a similar ozone reactivity as viruses ($k_{O3,CBZ}$ = 5.5 x $10^5$ $M^{-1}$ $s^{-1}$) (Wolf et al., 2018). Therefore, CBZ was chosen as second proxy for virus inactivation in this study.

The objectives of this study were (1) to investigate the influence of natural matrices on inactivation kinetics and $k_{O3\text{-}Virus}$, (2) to evaluate potential proxies (abatement of $UV_{254}$ or CBZ) for virus inactivation

during ozonation of environmental matrices, and (3) to validate these proxies for virus inactivation in a pilot-scale ozonation reactor. We used MS2 coliphage and an environmental strain of coxsackievirus B5 (CVB5) as model organisms. These viruses were selected because they exhibited different $k_{O3\text{-}Virus}$ in buffered solutions, and thus spanned a range of possible second order inactivation rate constants (Wolf et al., 2018). Furthermore, MS2 inactivation has previously been correlated to changes of $UV_{254}$ by *Gerrity et al*. (Gerrity et al., 2012), which enabled a comparison with previous results.

# 2. Materials and Methods

## 2.1. Chemicals and solutions

Sodium chloride (NaCl), monosodium phosphate ($NaH_2PO_4$) and disodium phosphate ($Na_2HPO_4$) were purchased from Acros. Ortho-phosphoric acid 85% ($H_3PO_4$,) was purchased from Fluka. Carbamazepine ($C_{15}H_{12}N_2O$), trans-cinnamic acid ($C_6H_5CHCHCOOH$), benzaldehyde ($C_7H_6O$) and 1 M HCl were purchased from Sigma-Aldrich. HPLC grade solvents were purchased from Biosolve chimie SARL. Indigo trisulfonate was purchased from Sigma.

## 2.2. Virus propagation, purification and enumeration

Coliphage MS2 (DSMZ 13767) and its host *Escherichia coli* (DSMZ 5695) were purchased from the German Collection of Microorganisms and Cell Cultures (DSMZ, Braunschweig, Germany). MS2 phages were propagated and purified using a polyethylene glycol (PEG)-chloroform method, as described previously (Pecson et al., 2009), except for the pilot experiment, where MS2 stocks were used without purification.

An environmental strain of the human enteric coxsackievirus B5 (CVB5) was isolated from the Vidy wastewater treatment plant (Lausanne, Switzerland), which is described elsewhere (Meister et al., 2018). CVB5 was propagated on buffalo green monkey kidney (BGMK) cells. BGMK cells were cultivated in minimum essential medium (MEM; Invitrogen), which was supplemented with penicillin (20 U $mL^{-1}$; Invitrogen), streptomycin (20 µg $mL^{-1}$; Invitrogen), and 2 or 10% fetal bovine serum (FBS; Invitrogen), and the cells were incubated at 37°C in 5% $CO_2$ and 95% humidity. Viruses were purified with the PEG-chloroform method.

All virus stock solutions were stored in phosphate buffered saline (PBS; 5 mM $NaH_2PO_4$, 10 mM NaCl, pH=7.5) at 4°C. Phages were enumerated by the double-agar-layer method as described previously (Pecson et al., 2009) and infective phage concentrations are expressed in plaque forming units (PFU)/mL. Enteric viruses were enumerated by the most probable number (MPN) assay as detailed elsewhere (Carratala Ripolles et al., 2015) and concentrations are expressed as most probable number of cytopathic units (MPNCU)/mL.

## 2.3. Water matrices

Virus ozonation was studied in two surface waters (SW) that serve as drinking water sources, and in a secondary wastewater (WW) effluent (Table 1). Surface waters were obtained from Lake Geneva (SWG; St-Sulpice, Switzerland) and Lac de Bret (SWB; Puidoux, Switzerland) and were collected at the intake of the local drinking water treatment plants. Secondary wastewater effluent (WW) was obtained from the wastewater treatment plant in Dübendorf, Switzerland. The water samples (30 L) were filtered through a 0.45 µm filter (PES, Merck Millipore Ltd.) and stored at 4°C in the dark until used. Details pertaining to the composition of the three water matrices are provided in Table 1. The dissolved organic carbon (DOC) was measured by catalytic combustion at 720 °C, followed by IR detection of $CO_2$ (Shimadzu TOC-L CSH). This method had a limit of quantification (LOQ) of 0.5 mgC/L, a range of 0.5-10 mgC/L and a measuring

error of 0.2 mgC/L. Alkalinity was determined by titration with HCl (0.1 mol/L; Metrohm 809 Titrando), with a LOQ and measuring error of 0.2 mM and 0.1 mM, respectively. For $NO_2^-$, a spectrophotometric determination of nitrite-nitrogen after the reaction to a reddish azo-dye (Griess reaction) was used (Griess, 1879). The corresponding LOQ was 1 µg/L, the measurement range was 1-20 µg/L, and the measuring error was 0.5 µg/L.

## 2.4. Ozone production

An ozone generator (Innovatec; model CMG 3-3/CMG 3-5, Rheinbach, Germany) was used to generate ozone gas from pure oxygen (99.999%, Carbagaz). The resulting ozone/oxygen mixture was sparged through Nanopure (Barnstead Nanopure, Thermofisher) or MilliQ (Millipore) ice cooled water (von Gunten and Hoigné, 1994). Concentrations of the ozone stock solutions ranged from 0.8 to 1.25 mM as determined by direct spectrophotometry with a molar absorption coefficient for ozone of $\varepsilon_{260} = 3200\ M^{-1}\,cm^{-1}$ (von Sonntag and von Gunten, 2012).

## 2.5. $O_3$ exposure measurements

Ozone exposures in SWB and WW were determined as a function of the specific ozone dose. Specifically, ozone depletion profiles were measured in SWB and WW for a range of specific ozone doses (0.01-0.9 and 0.04-1.5 $mgO_3/mgDOC$, respectively). The integration of the ozone depletion profile over time yielded the ozone exposure (von Gunten and Hoigné, 1994). Depletion profiles for low specific ozone doses were measured by quench-flow as described below. For higher specific ozone doses, the initial part of the depletion profile (up to 0.5 $mgO_3/mgDOC$) were measured by quench-flow and the later parts by the indigo method described below. The measured $O_3$ depletion profiles are shown in the supplementary information (SI, Figures S1-2). Because of the low DOC content of SWG, the applied ozone doses to achieve the desired range of specific $O_3$ doses were very low, and $O_3$ depletion profiles

were difficult to measure due to experimental limitation in the quench flow system (ozone consumption in tubing, LOQs for ozone determination by cinnamic acid). Therefore, the dependence of the ozone exposure on the specific ozone dose was not assessed for SWG.

*Measurement of ozone depletion profiles by quench-flow.* An $O_3$-containing feed solution (22- 968 µM) was mixed into water matrices with a mixing ratio of 10% to yield different specific ozone doses ranging from 0.01 to 0.6 or 0.04 to 0.6 $mgO_3$/mgDOC for SWB or WW, respectively. Ozone was quenched after defined contact times by mixing the sample at a 10:1 ratio with 100 mM cinnamic acid (CA) in Nanopure water at pH ~7. The quenched samples were collected in a syringe, and were used to determine benzaldehyde concentrations by HPLC as described previously (Wolf et al., 2018). Benzaldehyde is produced from the reaction of CA with ozone in a 1:1 stoichiometry, wherefore, its concentration in the quenched sample corresponds to the residual ozone concentration. For each specific ozone dose, the residual ozone concentration was measured at different time points to establish an ozone depletion curve versus time. Based on this data, ozone exposures were calculated using the *auc()* function ("catTools") (Tuszynski, 2014) in R (R Core Team (2016), 2016). The decay in the ozone feed solution over the course of the experiment was in the range of 1-5 %.

*Measurement of ozone depletion profiles in a batch system.* $O_3$ was spiked into 500 mL Schott bottles with a dispenser (Hoigné and Bader, 1994) to achieve specific ozone doses in the range of 0.25 to 0.86 $mgO_3$/mgDOC for SWB and 0.75 to 1.5 $mgO_3$/mgDOC for WW. Samples were withdrawn periodically from 30 s to 60 min and were added to an indigo quenching solution (0.1-1 mM) (Hoigné and Bader, 1994). For shorter time ranges (5 to 15 s), smaller reactors (10 mL) were used and the Indigo solution was added directly and under constant mixing (650rpm) into the vials to quench the residual ozone. The difference in absorbance at 600 nm was used to determine the residual $O_3$ concentration as described previously (Bader and Hoigné, 1981).

## 2.6. Inactivation experiments

The inactivation experiments of MS2 and CVB5 in the three matrices tested were performed in 50 mL or 100 mL glass batch reactors. MS2 or CVB5 were spiked to 400-500 mL of the water matrix under consideration at room temperature (22 ± 2°C) to yield initial concentrations of $10^8$ -$10^9$ PFU/mL for MS2 and $10^4$ -$10^6$ MPNCU/mL for CVB5, respectively. Ozone was then added to reach specific ozone doses ranging from 0.01-0.25 $mgO_3$/mgDOC for SWG, 0.01 to 0.58 $mgO_3$/mgDOC for SWB and 0.04 to 1 $mgO_3$/mgDOC for WW. During the addition of ozone, the reactors were mixed for 30 s, and were then kept at room temperature without further stirring for 1 hour, until all $O_3$ had been consumed. Aliquots were then withdrawn and the concentrations of residual infective viruses were determined.

## 2.7. Experiments with proxies

The abatement of proxies was quantified as $[CBZ]/[CBZ]_0$ or $UV_{254}/UV_{254,0}$, whereby the subscript « 0 » indicates the initial CBZ concentration or $UV_{254}$. In the high DOC matrices (SWB and WW), the abatement of CBZ and $UV_{254}$ were measured in the same experimental reactors as the inactivation of viruses. CBZ was spiked into a subset of batch reactors at concentrations between 0.67-0.9 µM in SWB and 0.88-1.02 µM in WW. These CBZ concentrations did not affect $UV_{254}$ of the matrix and did not alter the ozone exposure for the applied specific ozone doses. The CBZ concentration and $UV_{254}$ in each reactor before the addition of $O_3$ and after complete $O_3$ consumption were measured by HPLC-UV and spectrophotometry, respectively, as described previously (Wolf et al., 2018).

To investigate the use of CBZ as proxy for virus inactivation in SWG, a lower concentration of CBZ (0.04 µM) was used to prevent an increase in the ozone demand of the water. SWG has the lowest DOC concentration of the selected waters and higher concentrations may affect the ozone chemistry in this water. After the experiment, the remaining CBZ was quantified by online solid phase extraction followed

by ultra-performance liquid chromatography and tandem mass spectrometry (UPLC-MS/MS; Xevo TQ MS, Waters). Samples were diluted 1:1 with acidified Evian water (pH 2.5) and deuterated CBZ compounds were spiked to every sample as internal standards. The analytical method was adapted from previous work (Margot, 2015; Morasch et al., 2010), and details are given in the SI. $UV_{254}$ in SWG samples was measured using a 10 cm quartz cuvette.

A summary of all batch experiments conducted is given in the SI (Table S2).

## 2.8. Pilot experiment

The potential of $UV_{254}$ or CBZ abatement as proxies was validated in a pilot-scale ozonation reactor operated at the Lengg drinking water treatment plant (Zürich, Switzerland). The detailed setup of the pilot plant is described elsewhere (Bourgin et al., 2017). Briefly, Lake Zürich water (DOC =1.4 - 1.6 mg/L) was spiked with MS2 to a concentration of approximately $10^6$ PFU/mL. The water was then treated in an ozone reactor with a volume of 2 $m^3$ on two consecutive days. The reactor was operated at a flow rate of 10 $m^3$/h, and two ozone concentrations (0.3 $mgO_3$/L or 0.8 $mgO_3$/L), resulting in specific ozone doses of 0.2 or 0.5 $mgO_3$/mgDOC (SI, Table S3). Water samples (100 mL) were taken prior to ozone addition, immediately after ozone addition, at four points along the ozone reactor, as well as at the reactor effluent (details in the SI, Table S4). Residual ozone was quenched using 1 mL of 1.5 M sodium thiosulfate (Sigma) (for proxy and MS2 analysis) or by an indigo solution (to quantify ozone) (Bader and Hoigné, 1981). An unquenched effluent sample was used to measure $UV_{254}$ after complete ozone depletion.

The $O_3$ exposure in the reactor, which operates as a plug flow reactor (Kaiser et al., 2013), was determined based on the retention time (Bourgin et al., 2017) and the measured $O_3$ concentration at each sampling point (details in SI, Figure S3). $UV_{254}$ was determined in a 10 cm cuvette. CBZ abatement

was quantified using solid phase extraction, followed by UPLC-MS as described elsewhere (Morasch et al., 2010). For MS2 enumeration, the samples were concentrated 50-fold using a 100 kD Amicon filter (Millipore).

## 2.9. Data analysis

Data analysis was performed in R (R Core Team (2016), 2016). An R function was programed to compute the ozone exposure for each specific ozone dose by integration of the ozone decay curve versus time. This function used the packages "caTools" (Tuszynski, 2014) and "flux" (Jurasinski et al., 2014). The "*ggplot2*"(Wickham, 2009) and "*ggmcmc*"(Fernández i Marín, 2016) packages were used to draw graphics. Bayesian model selection (BMA) (Clyde et al., 2011) was performed using the BAS package (Clyde, 2018).

Bayesian analyses were performed using the "runjags"(Derwood, 2016) package, which interfaces with the Jags (Plummer, 2017) software, using Markov chain Monte Carlo sampling. Censored inactivation data and detection limits were incorporated into the analyses formulated with Jags as described elsewhere (Kruschke, 2010). Detection limits were determined according to the maximal measurable inactivation in each individual experiment. Parameter estimates were assumed to be normally distributed, and prior knowledge of mean values and standard deviations obtained from literature, were included (Carvajal et al., 2017; Gamage et al., 2013). When no prior knowledge was available, a non-informative normal prior or flat prior were used for the mean, and a uniform flat prior for the standard deviation. The number of simulations was set to $10^5$, of which the first $10^4$ were considered as the burn-in. Visual inspection of traceplots, plots and Geweke's diagnostics confirmed convergence of chains. Diagnostics plots were constructed using the *"ggmcmc"* (Fernández i Marín, 2016) and *"coda"* (Plummer et al., 2006) packages (data not shown).

# 3. Results and Discussion

## 3.1. Virus inactivation, $UV_{254}$ and CBZ abatement as a function of the specific ozone dose

Figure 1 shows the negative of the natural log (ln) of the relative abatement of viruses (MS2 and CVB5), $UV_{254}$ or CBZ as a function of the specific ozone dose for SWS, SWB and WW (from left to right). Generally, the effects of the specific ozone dose on virus infectivity, $UV_{254}$ and CBZ were quite similar in the two SWs, and to lesser extent in WW. Given that the DOC content in SWB was close to that in WW but higher than in SWG, this indicates that the effects of ozonation, when normalized as the specific ozone dose, depends more on the type of water (and hence dissolved organic matter (DOM)) than on the DOC concentration.

Infective viruses could be measured up to specific ozone doses of 0.5 $mgO_3$/mgDOC, beyond which inactivation rapidly exceeded the limits of quantification. Inactivation exhibited an approximately log-linear trend versus specific ozone dose for all waters tested, and was similar for both viruses considered. Both SWs tested exhibited similar trends, whereas inactivation in WW proceeded more gradually. The inactivation of MS2 in WW roughly corresponded to that reported by Gamage et al. (2013) in five filtered WWs of different origin and different DOC content (SI, Figure S4) (Gamage et al., 2013). However, in this study the minimal specific ozone dose was 0.25 $mgO_3$/mg total organic carbon (TOC), and thus mainly very high levels of inactivation were observed.

$UV_{254}$ abatement exhibited similar dependences on the specific ozone dose for the two SWs considered. The trend in WW matched that reported for different WWs by Gamage et al. (2013) (SI, Figure S5) (Gamage et al., 2013). In previous studies (Carvajal et al., 2017; Gamage et al., 2013; Gerrity et al., 2012), the relationship between $UV_{254}$ abatement and the specific ozone dose was described by a power function, and such a function also fits the data reported herein.

CBZ abatement in all waters tested exhibited a lag phase at low specific ozone doses. This lag phase was particularly pronounced in WW, and may be explained by competition with reactive moieties of the dissolved organic matter (DOM) with a higher reactivity towards ozone than CBZ ($k_{O3,CBZ}$ = 5.5 x $10^5$ $M^{-1}$ $s^{-1}$) (Wolf et al., 2018). Hence, at very low specific doses, ozone is preferentially consumed by DOM, resulting in a reduced CBZ abatement. Once the moieties with the highest reactivities (e.g., phenols, $k_{app,O3}$ > $10^7$ $M^{-1}s^{-1}$) (Hoigné and Bader, 1983; Önnby et al., 2018) are oxidized (at specific ozone doses of approximately 0.07 and 0.15 $mgO_3$/mgDOC for SWs or WW, respectively), residual ozone is available for the abatement of CBZ. A lag-phase was also observed by Lester *et al.*(Lester et al., 2013), who reported similar abatement of CBZ as a function of specific ozone dose in WW (SI, Figure S6). In contrast, no lag-phase was observed by Chon *et al.* (Chon et al., 2015), because they applied higher specific ozone doses, with the lowest dose above the range for which a lag phase could be observed.

## 3.2. Virus inactivation, $UV_{254}$ and CBZ abatement as a function of the ozone exposure

To determine if the different responses of virus inactivation, $UV_{254}$ and CBZ to ozonation in SW and WW could be rationalized by the water matrix-dependent ozone exposures resulting from the different specific ozone doses were determined for SWB and WW (Figure 2). The corresponding ozone depletion curves for the different specific ozone doses applied are shown in the SI (Figures S1 and S2). The measured ozone exposures ranged from $10^{-7}$ to $10^{-2}$ Ms, with very low exposures (< $10^{-4}$ Ms) resulting from doses of up to 0.1 and 0.3 $mgO_3$/mgDOC in SWB and WW respectively, followed by a rapid increase (Figure 2). The ozone exposure was higher in SWB than in WW for similar specific ozone doses in the range tested. This demonstrates again the higher ozone demand of WW compared to SWB.

The upper range of ozone exposures in WW corresponded well to those measured by Gamage *et al.* (SI, Figure S7) (Gamage et al., 2013). These authors proposed a linear dependence of ozone exposure on the specific ozone dose, though such a dependence does not apply to the lower doses considered herein. In

another study, the ozone exposure was fitted as a logarithmic function of the specific ozone dose (Lee et al., 2014). In the current study, this relationship was not satisfactory (Figure 2a), therefore, the relationship between the specific ozone dose and resulting ozone exposure was fitted using the following function:

$$ln\,(O_3\ exposure) = a * \ln(specific\ \ O_3\ dose) + b \qquad \text{Equation 1}$$

The modeled parameters *a* and *b* and associated statistics are given in Table 2.

Based on these models, the ozone exposure can be estimated for any specific ozone dose in these waters (Figure 2b). The data for virus inactivation, $UV_{254}$ abatement and CBZ abatement shown in Figure 1 could thus be re-evaluated as a function of the ozone exposure (Figure 3).

Virus inactivation curves exhibited a rapid initial decrease in infective virus concentrations at low exposures, followed by a pronounced tailing (Figures 3a and b). MS2 and CVB5 exhibited similar kinetics versus exposure and were detectable up to an exposure of 1.15 x $10^{-5}$ and 1.14 x $10^{-3}$ Ms in SWB, respectively, compared to 2.3 x $10^{-3}$ to 8.75 x $10^{-3}$ Ms in WW. Beyond these exposures, the inactivation exceeded the measurable inactivation range of 9 $\log_{10}$ (20.7 ln) for MS2 and 5 $\log_{10}$ (11.5 ln) for CVB5. Inactivation was generally lower in WW than in SWB for similar exposures, indicating that matrix constituents, such as small particles that passed through the 0.45 µm filter, have a protective effect on the virus (Templeton et al., 2008).

Matrix effects were also apparent when comparing the inactivation curves in SW and WW to those in homogeneous buffer solutions. The solid lines in Figure 3 represent inactivation curves predicted based on kinetic modeling with second order rate constants for the virus inactivation ($k_{O3\text{-}MS2}$ = 1.9 x $10^6$ $M^1s^{-1}$; $k_{O3\text{-}CVB5}$ = 4.4 x $10^5$ $M^1s^{-1}$) determined in buffered solutions (Wolf et al., 2018). In these pure water systems, inactivation was measured up to ozone exposures of 1 x $10^{-5}$ Ms, which corresponds to an

292 inactivation of up to 8.2 or 2.2 $log_{10}$ for MS2 or CVB5, respectively. For CVB5, this prediction corresponds
293 reasonably well to the observed inactivation in SWB and WW in the comparable range. In contrast, MS2
294 inactivation is well estimated in the fast, initial phase in SWB, but rapidly overestimates the inactivation
295 in WW. This highlights that inactivation kinetics determined in model systems have some value for
296 estimating virus inactivation during treatment of real matrices: they can predict the log-linear portion of
297 the inactivation in real water matrices, but fail to consider the tail at higher ozone exposures, which
298 likely results from protective effects of different matrix constituents.

299 The dependence of $UV_{254}$ on ozone exposure (Figure 3c) exhibited a similar trend as virus inactivation,
300 with a rapid initial decrease in $UV_{254}$, followed by a slower decrease at higher exposures. This trend
301 reflects the reaction of ozone with DOM: at low specific ozone doses, ozone is rapidly consumed by
302 reactive organic moieties of WW DOM (e.g., phenolic moieties), which also absorb UV light (Chon et al.,
303 2015; Önnby et al., 2018). This results in a very low ozone exposure (Figure 2), but significant decrease in
304 $UV_{254}$. At higher doses, when most fast-reacting moieties are oxidized, the consumption of ozone and
305 associated decrease in $UV_{254}$ slow down, while the ozone exposure still increases. In SW, the abatement
306 of $UV_{254}$ slows down at lower ozone exposures compared to WW, indicating the presence of fewer
307 ozone-reactive organic moieties.

308 CBZ abatement exhibited a roughly log-linear dependence on ozone exposure. In both water types, the
309 abatement kinetics were similar and corresponded reasonably well to those predicted based on the
310 second order rate constant for CBZ abatement determined in buffer solutions (Wolf et al., 2018). In
311 WW, however, some scatter in the data was observed, with two measurements yielding a lower
312 abatement than expected.

### 3.3. Correlations between virus inactivation and the specific ozone dose, $UV_{254}$ or CBZ abatement

Virus inactivation was cross-correlated with the abatement of $UV_{254}$ or CBZ, to evaluate their utility as proxies (Figure 4). Virus inactivation in SWG and SWB exhibited a roughly linear correlation between $\ln(N/N_0)$ and $\ln (UV_{254}/UV_{254,0})$, though in WW, a lag-phase was observed up to a $\ln (UV_{254}/UV_{254,0})$ of 0.2 (Figure 2a). Reaction of ozone with highly reactive moieties present in wastewater DOM, may explain the initial abatement in $UV_{254}$ absorbance prior to the onset of inactivation. The relationship between $UV_{254}$ and inactivation obtained in WW corresponded well to that observed by Gerrity *et al.* (2012) (Figure S8). While none of their samples exhibited abatements in $UV_{254}$ < 15%, the trend at higher $UV_{254}$ abatements is comparable to the observations**Error! Reference source not found.** in this study. Interestingly, the data by Gerrity *et al. (2012*) includes five different wastewaters from various origins and with DOC concentrations ranging from 6.3 to 18 mg/L. Combined with the data obtained herein, this indicates that a single relationship between $UV_{254}$ abatement and virus inactivation applies across vastly different wastewaters. This is probably due to the fact that the DOM of wastewaters is quite similar across different wastewater treatment plants. This is further supported by the fact, that the abatement of micropollutants as a function of the specific ozone dose is similar for different wastewaters (Lee et al., 2013).

Inactivation as a function of the CBZ abatement exhibited a maximum of 5, 4 and 3 orders of magnitude in SWG, SWB and WW, respectively, before the limit of detection for CBZ abatement was reached (Figure 4b). This relationship exhibited a concave shape, which results from the CBZ abatement exhibiting a lag-phase at low ozone doses, whereas no lag phase was observed for virus inactivation (Figure 1).

## 3.4. Predictive relationships between proxies and virus inactivation

Given the reasonable correlations between measured virus inactivation and the two proxies (Figure 4), the proxies were used to develop predictive relationships to estimate virus inactivation in the absence of a measurement. A predictive relationship was also established based on the specific ozone dose, which also exhibited a strong correlation with inactivation (Figure 1). The specific ozone dose is not a traditional proxy, however, it may serve as an indicator of the inactivation achieved during treatment, in particular if all ozone is consumed during treatment, which is typical for wastewater ozonation.

To establish predictive relationships between the different proxies and virus inactivation, we first determined which system variables significantly contribute to explaining the observed variation in inactivation. To this end, we used Bayesian model averaging (BMA; see SI for details) (Clyde, 2018) considering four variables: virus species, water type (i.e., surface water or wastewater), DOC content, and the proxy under consideration. One result of BMA is the probability (p) that a given variable may be included in a model to explain the variation in the response variable. Furthermore, it gives an estimate of the effect size of each variable (SI, Figures S9-S11 and Tables S5-S7).

BMA results for the specific $O_3$ dose and for $UV_{254}$ abatement as a proxy show that the specific $O_3$ dose and $UV_{254}$, abatement are the variables with the greatest effect (10 and 12.5 per unit of proxy, respectively). Furthermore, the water type ($p \geq 0.98$) was also relevant, whereas the DOC concentration was not ($p << 0.95$), since it is already considered in the specific ozone dose. Finally, BMA identified the virus species as a relevant model variable ($p \geq 0.97$). However, given their similar inactivation rate constants, the effect is small and close to the experimental uncertainty of the infectivity assay (~0.5 $log_{10}$). Therefore, this variable was not included in the predictive model below. For CBZ abatement as a proxy, the BMA revealed no dependence of inactivation neither on virus species, nor water type, nor

357 DOC concentration. Hence, CBZ abatement is the only relevant variable needed to explain variation in
358 inactivation.

359 To establish predictive relationships between virus inactivation and proxies, we used a Bayesian model
360 structure that considers censored inactivation data. Proxy-inactivation relationships were modeled as a
361 power function (equation 2), to capture the deviations from linearity in the proxy-inactivation
362 correlations:

363 $$ln\left(\frac{N}{N_0}\right) = \gamma_0 * \left(Specific\ O_3\ dose\ OR\ \ln\left(\frac{[CBZ]}{[CBZ]_0}\right)\ OR\ \ln\left(\frac{UV_{254}}{UV_{254,0}}\right)\right)^{\gamma_1} \quad \text{Equation 2}$$

364 Because the water type was identified by the BMA as a relevant model variable when using the specific
365 $O_3$ dose or $UV_{254}$ as proxies, separate sets of model parameters were obtained for each water type. For
366 CBZ, SW and WW could be fit with the same model. Bayesian power model predictions, along with the
367 corresponding 95% credible intervals are shown in SI, Figure S12 for the two types of water and all
368 proxies studied. The model parameters for all proxies are summarized in Table 3.

369 Both the specific ozone dose and $UV_{254}$ abatement could predict inactivation of up to 8 or 5 orders of
370 magnitude in SW and WW, respectively, for an approximate 50% $UV_{254}$ reduction. In contrast, CBZ is
371 strongly abated during ozonation (Gerrity et al., 2012; Lee et al., 2014); as such, the range over which
372 virus inactivation may be estimated is limited by the initial concentration of CBZ and its limit of
373 quantification. In this study, virus inactivation could be predicted up to 4 orders of magnitude with CBZ
374 with good confidence both in SW and in WW.

375 For a specific $O_3$ dose of 0.5 $mgO_3$/mgDOC, which is typical for micropollutant abatement in enhanced
376 WW treatment (Bourgin et al., 2018), the predicted inactivation in WW corresponds to 4.5 $log_{10}$ (95%CI:
377 1.9 to 7.2 $log_{10}$) or 10.5 ln (95%CI: 4.4 to 16.6 ln). Thus, this operational specific ozone dose will

inactivate the viral load by at least 2 orders of magnitude, and will more likely yield around 4.5 orders of magnitude of inactivation.

As a validation for the specific ozone dose and $UV_{254}$ as proxies, a prediction of the MS2 inactivation in WW reported by Gerrity *et al.* (2012) and Gamage *et al.* (2013) was performed. Figure 5 shows the inactivation predicted by Equation 2 (black line) together with credible intervals and the measured inactivation as a function of (a) the specific ozone dose or (b) $\ln(UV_{254}/UV_{254,0})$. The model predictions are in reasonable agreement with the measured inactivation data (symbols). Since the data of Gerrity *et al*. (2012) and Gamage *et al.* (2013) comprise five different wastewaters, the good model predictions established herein confirm that the proxy-inactivation relationships in wastewater are robust and can be applied over a wide range of DOC concentrations.

## 3.5. Proxy validation in a pilot-scale ozonation reactor

The applicability of the developed proxy-inactivation relationships for MS2 was validated in a pilot-scale ozonation reactor described elsewhere (Bourgin et al., 2017; Kaiser et al., 2013). This pilot reactor treats water from Lake Zurich and was operated at two specific ozone doses of 0.2 and 0.6 $mgO_3$/mgDOC (see SI, Tables S3 and S4 for details).

Figure 6a shows the MS2 inactivation throughout the ozonation reactor as a function of the ozone exposure. Residual infective MS2 concentrations could be measured throughout the reactor and in the reactor effluent for the lower specific ozone dose of 0.2 $mgO_3$/mgDOC (red circles, Fig. 6a). Because most of the ozone was consumed between the influent and sampling point P1 (see SI, Figure S3 for the location of the points), both the ozone exposure and MS2 inactivation increased only slowly beyond this point. For the higher specific ozone dose (0.6 $mgO_3$/mgDOC), infective MS2 concentrations could be measured up to sampling point P3.

Figures 6b-d show the measured inactivation of MS2 as a function of the three proxies evaluated in this study. The predicted inactivation by the different proxy-inactivation relationships for SW developed herein is also shown (black lines). Predictions could only be experimentally validated for a specific ozone dose of 0.2 $mgO_3$/mgDOC. For the higher specific ozone dose (0.6 $mgO_3$/mgDOC), CBZ concentrations were below the detection limit in all treated samples, and MS2 was not detectable in the effluent sample in which $UV_{254}$ was determined. As is shown in Figures 6b-d, the observed inactivation fell well within the predicted range for all proxies tested. This confirms that the predictive models developed in batch systems herein for a similar water type (SW) can also be applied to a flow-through pilot plant if the reactor hydraulics are known.

# 4. Conclusions

We tested the specific ozone dose, $UV_{254}$ and carbamazepine (CBZ) abatement for their applicability to predict or monitor virus (MS2 and CVB5) inactivation during ozonation. These proxies allowed to estimate virus inactivation over several orders of magnitude. For the specific $O_3$ dose or $UV_{254}$ abatement, single proxy-inactivation relationships could be applied to both MS2 and CBV5, but depended on the water type. In contrast, a single proxy-inactivation relationship for CBZ abatement could be applied across all waters and both viruses tested.

Each proxy tested comes with a set of advantages and limitations. The main advantages of the specific $O_3$ dose is that it does not require any specialized monitoring equipment, and is able to predict a wide range of virus inactivation. Its main limitation is that it can only be used to predict the overall inactivation, but not to monitoring inactivation during ozonation treatment. Therefore, it cannot detect unexpected anomalies during ozonation. In contrast, $UV_{254}$ abatement is already used to monitor the micropollutant abatement efficiency in wastewater treatment plants, and therefore, its utility could

423 easily be expanded to indirect real-time assessment of virus inactivation. A limitation of $UV_{254}$
424 abatement is that this proxy may be challenging to apply in low DOC waters, where the initial
425 absorbance is low. The use of CBZ as a proxy necessitates that the water matrix under consideration
426 contains sufficient CBZ such that it can be quantified prior to and during ozonation. CBZ concentrations
427 are typically low, therefore, the range of inactivation over which this proxy can be applied is likely
428 narrow. In addition, CBZ measurements require the use of specialized analytical equipment as well as
429 considerable sample work-up. However, this proxy has the advantage that it is independent of the water
430 type, such that it may be applied to any matrix of interest. Finally, a potential limitation common to all
431 proxies is their utility in waters containing many particles. The proxy-inactivation relationships reported
432 herein as well as in previous studies were developed in matrices containing few particles (filtered raw
433 drinking water or secondary wastewater effluent). Because particles are known to shield pathogens
434 from disinfectants, these relationships may only apply to a narrow range of inactivation, or may break
435 down entirely, in matrices with a higher particle content (e.g., primary wastewater effluent). For such
436 water types, the proxy-inactivation relationships thus remain to be validated.

437

438 # 5. Acknowledgements

439 This study was funded by the Swiss National Science Foundation (Grant No. 205321_169615). Elisabeth
440 Salhi, Loïc Decrey, Dominique Grandjean and Jakob Helbing are acknowledged for help in the laboratory
441 and/or on the pilot plant.

442

# 6. References

Bader, H., Hoigné, J., 1981. Determination of ozone in water by the indigo method. Water Res. 15, 449–456. https://doi.org/10.1016/0043-1354(81)90054-3

Bahr, C., Schumacher, J., Ernst, M., Luck, F., Heinzmann, B., Jekel, M., 2007. SUVA as control parameter for the effective ozonation of organic pollutants in secondary effluent. Water Sci. Technol. 55, 267–274. https://doi.org/10.2166/wst.2007.418

Bicknell, D.L., Jain, R.K., 2001. Ozone disinfection of drinking water — technology transfer and policy issues. Environ. Eng. Policy 3, 55–66. https://doi.org/10.1007/s100220100043

Bourgin, M., Beck, B., Boehler, M., Borowska, E., Fleiner, J., Salhi, E., Teichler, R., von Gunten, U., Siegrist, H., McArdell, C.S., 2018. Evaluation of a full-scale wastewater treatment plant upgraded with ozonation and biological post-treatments: Abatement of micropollutants, formation of transformation products and oxidation by-products. Water Res. 129, 486–498. https://doi.org/10.1016/j.watres.2017.10.036

Bourgin, M., Borowska, E., Helbing, J., Hollender, J., Kaiser, H.-P., Kienle, C., McArdell, C.S., Simon, E., von Gunten, U., 2017. Effect of operational and water quality parameters on conventional ozonation and the advanced oxidation process O3/H2O2: Kinetics of micropollutant abatement, transformation product and bromate formation in a surface water. Water Res. 122, 234–245. https://doi.org/10.1016/j.watres.2017.05.018

Buffle, M.-O., Schumacher, J., Meylan, S., Jekel, M., von Gunten, U., 2006a. Ozonation and Advanced Oxidation of Wastewater: Effect of O3 Dose, pH, DOM and HO•-Scavengers on Ozone Decomposition and HO• Generation. Ozone Sci. Eng. 28, 247–259. https://doi.org/10.1080/01919510600718825

Buffle, M.-O., Schumacher, J., Salhi, E., Jekel, M., von Gunten, U., 2006b. Measurement of the initial phase of ozone decomposition in water and wastewater by means of a continuous quench-flow

system: Application to disinfection and pharmaceutical oxidation. Water Res. 40, 1884–1894. https://doi.org/10.1016/j.watres.2006.02.026

Carratala Ripolles, A., Dionisio Calado, A., Mattle, M.J., Meierhofer, R., Luzi, S., Kohn, T., 2015. Solar disinfection (SODIS) of viruses in PET bottles. Appl. Environ. Microbiol. 279–88. https://doi.org/10.1128/AEM.02897-15

Carvajal, G., Branch, A., Michel, P., Sisson, S.A., Roser, D.J., Drewes, J.E., Khan, S.J., 2017. Robust evaluation of performance monitoring options for ozone disinfection in water recycling using Bayesian analysis. Water Res. 124, 605–617. https://doi.org/10.1016/j.watres.2017.07.079

Chon, K., Salhi, E., von Gunten, U., 2015. Combination of UV absorbance and electron donating capacity to assess degradation of micropollutants and formation of bromate during ozonation of wastewater effluents. Water Res. 81, 388–397. https://doi.org/10.1016/j.watres.2015.05.039

Clyde, M., 2018. BAS: Bayesian Variable Selection and Model Averaging using Bayesian Adaptive Sampling.

Clyde, M.A., Ghosh, J., Littman, M.L., 2011. Bayesian Adaptive Sampling for Variable Selection and Model Averaging. J. Comput. Graph. Stat. 20, 80–101.

Derwood, M.J., 2016. Runjags: An R Package Providing Interface Utilities, Model Templates, Parallel Computing Methods and Additional Distributions for MCMC Models in JAGS. Journal of Statistical Software 71, 1–25. https://doi.org/doi:10.18637/jss.v071.i09

Eggen, R.I.L., Hollender, J., Joss, A., Schärer, M., Stamm, C., 2014. Reducing the discharge of micropollutants in the aquatic environment: The benefits of upgrading wastewater treatment plants. Environ. Sci. Technol. 48, 7683–7689. https://doi.org/10.1021/es500907n

Farkas, K., Cooper, D.M., McDonald, J.E., Malham, S.K., de Rougemont, A., Jones, D.L., 2018. Seasonal and spatial dynamics of enteric viruses in wastewater and in riverine and estuarine receiving waters. Sci. Total Environ. 634, 1174–1183. https://doi.org/10.1016/j.scitotenv.2018.04.038

491 Fernández i Marín, X., 2016. ggmcmc : Analysis of MCMC Samples and Bayesian Inference 70, 1–20.
492 https://doi.org/10.18637/jss.v070.i09
493 Gamage, S., Gerrity, D., Pisarenko, A.N., Wert, E.C., Snyder, S.A., 2013. Evaluation of Process Control
494 Alternatives for the Inactivation of Escherichia coli, MS2 Bacteriophage, and Bacillus subtilis
495 Spores during Wastewater Ozonation. Ozone Sci. Eng. 35, 501–513.
496 https://doi.org/10.1080/01919512.2013.833852
497 Gerrity, D., Gamage, S., Jones, D., Korshin, G.V., Lee, Y., Pisarenko, A., Trenholm, R.A., von Gunten, U.,
498 Wert, E.C., Snyder, S.A., 2012. Development of surrogate correlation models to predict trace
499 organic contaminant oxidation and microbial inactivation during ozonation. Water Res. 46,
500 6257–6272. https://doi.org/10.1016/j.watres.2012.08.037
501 Gerrity, D., Pecson, B.M., Trussell, R.S., Trussell, R.R., 2013. Potable reuse treatment trains throughout
502 the world. AQUA 62, 321–338. https://doi.org/DOI: 10.2166/aqua.2013.041
503 Griess, P., 1879. Bemerkungen zu der Abhandlung der HH. Weselsky und Benedikt „Ueber einige
504 Azoverbindungen”□. Berichte Dtsch. Chem. Ges. 12, 426–428.
505 https://doi.org/10.1002/cber.187901201117
506 Hoigné, J., Bader, H., 1994. Characterization Of Water Quality Criteria for Ozonation Processes. Part II:
507 Lifetime of Added Ozone. Ozone Sci. Eng. 16, 121–134.
508 https://doi.org/10.1080/01919519408552417
509 Hoigné, J., Bader, H., 1983. Rate constants of reactions of ozone with organic and inorganic compounds
510 in water—I. Water Res. 17, 173–183. https://doi.org/10.1016/0043-1354(83)90098-2
511 Jurasinski, G., Koebsch, F., Guenther, A., Beetz, S., 2014. Flux rate calculation from dynamic closed
512 chamber measurements. R package version 0.3-0.

513 Kaiser, H.-P., Köster, O., Gresch, M., Périsset, P.M.J., Jäggi, P., Salhi, E., Gunten, U. von, 2013. Process
514 Control For Ozonation Systems: A Novel Real-Time Approach. Ozone Sci. Eng. 35, 168–185.
515 https://doi.org/10.1080/01919512.2013.772007
516 Kruschke, J.K., 2010. Doing Bayesian Data Analysis: A Tutorial with R and BUGS, 1st ed. Academic Press,
517 Inc., Orlando, FL, USA.
518 Lee, Y., Gerrity, D., Lee, M., Bogeat, A.E., Salhi, E., Gamage, S., Trenholm, R.A., Wert, E.C., Snyder, S.A.,
519 von Gunten, U., 2013. Prediction of micropollutant elimination during ozonation of municipal
520 wastewater effluents: Use of kinetic and water specific information. Environ. Sci. Technol. 47,
521 5872–5881. https://doi.org/10.1021/es400781r
522 Lee, Y., Kovalova, L., McArdell, C.S., von Gunten, U., 2014. Prediction of micropollutant elimination
523 during ozonation of a hospital wastewater effluent. Water Res. 64, 134–148.
524 https://doi.org/10.1016/j.watres.2014.06.027
525 Lester, Y., Mamane, H., Zucker, I., Avisar, D., 2013. Treating wastewater from a pharmaceutical
526 formulation facility by biological process and ozone. Water Res. 47, 4349–4356.
527 https://doi.org/10.1016/j.watres.2013.04.059
528 Lodder, W.J., de Roda Husman, A.M., 2005. Presence of Noroviruses and Other Enteric Viruses in
529 Sewage and Surface Waters in The Netherlands. Appl. Environ. Microbiol. 71, 1453–1461.
530 https://doi.org/10.1128/AEM.71.3.1453-1461.2005
531 Margot, J., 2015. Micropollutant removal from municipal wastewater - From conventional treatments to
532 advanced biological processes. Thesis N° 6505 EPFL.
533 Meister, S., Verbyla, M.E., Klinger, M., Kohn, T., 2018. Variability in Disinfection Resistance between
534 Currently Circulating Enterovirus B Serotypes and Strains. Environ. Sci. Technol. 52, 3696–3705.
535 https://doi.org/10.1021/acs.est.8b00851

536 Morasch, B., Bonvin, F., Reiser, H., Grandjean, D., De Alencastro, L.F., Perazzolo, C., Chèvre, N., Kohn, T.,
537 2010. Occurrence and fate of micropollutants in the Vidy Bay of Lake Geneva, Switzerland. Part
538 II: Micropollutant removal between wastewater and raw drinking water. Environ. Toxicol. Chem.
539 https://doi.org/10.1002/etc.222
540 OFEV, 2015. Qualité de l'eau : révision de l'ordonnance sur la protection des eaux.
541 Önnby, L., Salhi, E., McKay, G., Rosario-Ortiz, F.L., von Gunten, U., 2018. Ozone and chlorine reactions
542 with dissolved organic matter - Assessment of oxidant-reactive moieties by optical
543 measurements and the electron donating capacities. Water Res. 144, 64–75.
544 https://doi.org/10.1016/j.watres.2018.06.059
545 Pecson, B.M., Martin, L.V., Kohn, T., 2009. Quantitative PCR for determining the infectivity of
546 bacteriophage MS2 upon inactivation by heat, UV-B radiation, and singlet oxygen: advantages
547 and limitations of an enzymatic treatment to reduce false-positive results. Appl. Environ.
548 Microbiol. 75, 5544–5554. https://doi.org/10.1128/AEM.00425-09
549 Plummer, M., 2017. JAGS : Just another Gibbs sampler.
550 Plummer, M., Best, N., Cowles, K., Vines, K., 2006. CODA: Convergence Diagnosis and Output Analysis for
551 MCMC. R News 6, 7–11.
552 R Core Team (2016), 2016. R: A language and environment for statistical computing. Foundation for
553 Statistical Computing, Vienna, Austria.
554 Sigmon, C., Shin, G.-A., Mieog, J., Linden, K.G., 2015. Establishing surrogate–virus relationships for ozone
555 disinfection of wastewater. Environ. Eng. Sci. 32, 451–460.
556 https://doi.org/10.1089/ees.2014.0496
557 Stamm, C., Eggen, R.I.L., Hering, J.G., Hollender, J., Joss, A., Schärer, M., 2015. Micropollutant removal
558 from wastewater: facts and decision-making despite uncertainty. Environ. Sci. Technol. 49,
559 6374–6375. https://doi.org/10.1021/acs.est.5b02242

560 Templeton, M.R., Andrews, R.C., Hofmann, R., 2008. Particle-Associated Viruses in Water: Impacts on
561 Disinfection Processes. Crit. Rev. Environ. Sci. Technol. 38, 137–164.
562 https://doi.org/10.1080/10643380601174764
563 Ternes, T.A., Stüber, J., Herrmann, N., McDowell, D., Ried, A., Kampmann, M., Teiser, B., 2003.
564 Ozonation: a tool for removal of pharmaceuticals, contrast media and musk fragrances from
565 wastewater? Water Res. 37, 1976–1982. https://doi.org/10.1016/S0043-1354(02)00570-5
566 Tuszynski, J., 2014. caTools: Tools: moving window statistics, GIF, Base64, ROC AUC, etc. R package
567 version 1.17.1.
568 von Gunten, U., 2018. Oxidation Processes in Water Treatment: Are We on Track? Environ. Sci. Technol.
569 52, 5062–5075. https://doi.org/10.1021/acs.est.8b00586
570 von Gunten, U., Hoigné, J., 1994. Bromate formation during ozonization of bromide-containing waters:
571 interaction of ozone and hydroxyl radical reactions. Environ. Sci. Technol. 28, 1234–1242.
572 https://doi.org/10.1021/es00056a009
573 von Sonntag, C., von Gunten, 2012. Chemistry of Ozone in Water and Wastewater Treatment: From
574 Basic Principles to Applications. IWA publishing, London.
575 Wickham, H., 2009. ggplot2: Elegant Graphics for Data Analysis. New York.
576 Wolf, C., von Gunten, U., Kohn, T., 2018. Kinetics of Inactivation of Waterborne Enteric Viruses by
577 Ozone. Environ. Sci. Technol. 52, 2170–2177. https://doi.org/10.1021/acs.est.7b05111
578 World Health Organization, 2017. Potable reuse: Guidance for producing safe drinking-water.
579

Table 1. Water quality parameters of real water samples from Switzerland (SWG: Lake Geneva water; SWB: Lake de Bret water; WW: Wastewater effluent Dübendorf)

| Water | DOC [mgC/L] | $NO^-_2$ [µgN/L] | Alkalinity [mmol/L] | pH |
|---|---|---|---|---|
| **SWG** | 1.2 | < 1.0 | 1.77 | 8.2 |
| **SWB** | 5.2 | 10.8 | 3.6 | 8.2 |
| **WW** | 6.2 | 172.7 | 6.3 | 8.2 |

Table 2. Model parameters and relevant statistics for the $O_3$ exposure model as a function of the specific $O_3$ dose [$mgO_3$/mgDOC] for SWB and WW.

| Water | Model parameter | Estimate | p value | adjusted $R^2$ |
|---|---|---|---|---|
| **SWB** | a | 2.9 ± 0.16 | 2.34E-05 | 0.969 |
| | b | -3.4 ± 0.16 | 2.66E-08 | |
| | model | | 2.65E-08 | |
| **WW** | a | 3.74 ± 0.23 | 4.64E-07 | 0.9586 |
| | b | - 4.73 ± 0.41 | 1.90E-08 | |
| | model | | 1.90E-08 | |

Table 3. Summary of Bayesian model parameters for equation 2 for each proxy. Values indicate mean ± standard deviation. The 95% credible intervals are shown in parentheses.

**Specific $O_3$ dose**

| Water type | $\gamma_0$ | $\gamma_1$ |
|---|---|---|
| **SW** | 38 ± 2.6 (33, 43.4) | 0.7 ± 0.03 (0.6, 0.8) |
| **WW** | 18 ± 1.2 (16, 20.6) | 0.79 ± 0.06 (0.7, 0.9) |

**$UV_{254}$**

| Water type | $\gamma_0$ | $\gamma_1$ |
|---|---|---|
| **SW** | 25.1 ± 1.8 (21.7, 28.8) | 0.7 ± 0.06 (0.6, 0.8) |
| **WW** | 22 ± 1.9 (19, 26.6) | 1 ± 0.1 (0.8, 1.2) |

**CBZ abatement**

| Water type | $\gamma_0$ | $\gamma_1$ |
|---|---|---|
| **SW/WW** | 3.6 ± 0.2 (3.2, 4) | 0.5 ± 0.04 (0.4, 0.5) |

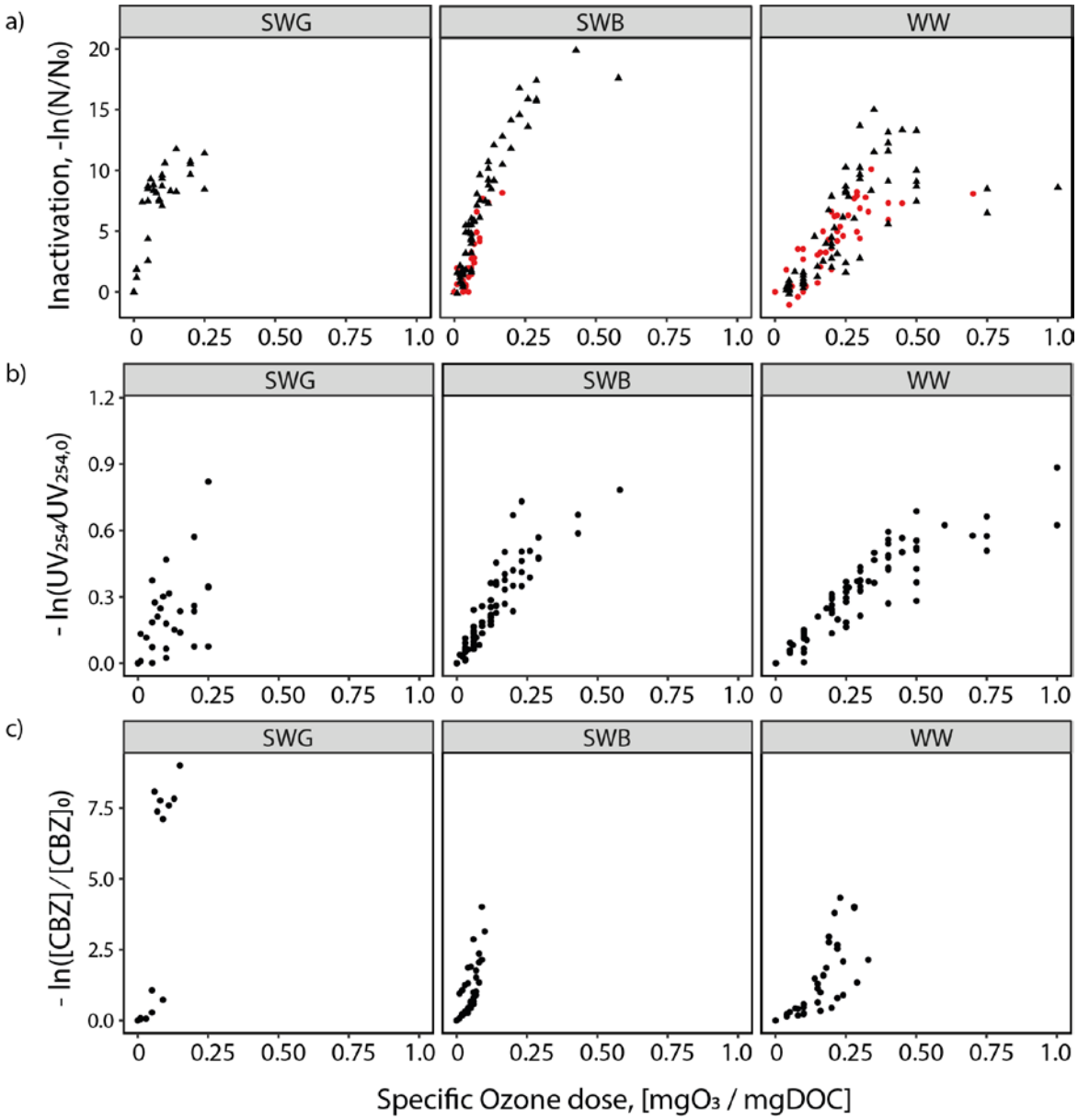


Figure 1. **Virus inactivation, $UV_{254}$ abatement and CBZ abatement as a function of the specific ozone dose**. a) Inactivation of MS2 (black triangles) and CVB5 (red dots) in the surface water of Lake Geneva (SWG) and Lake Bret (SWB), and secondary effluent wastewater (WW); b) $UV_{254}$ abatement; c) CBZ abatement.

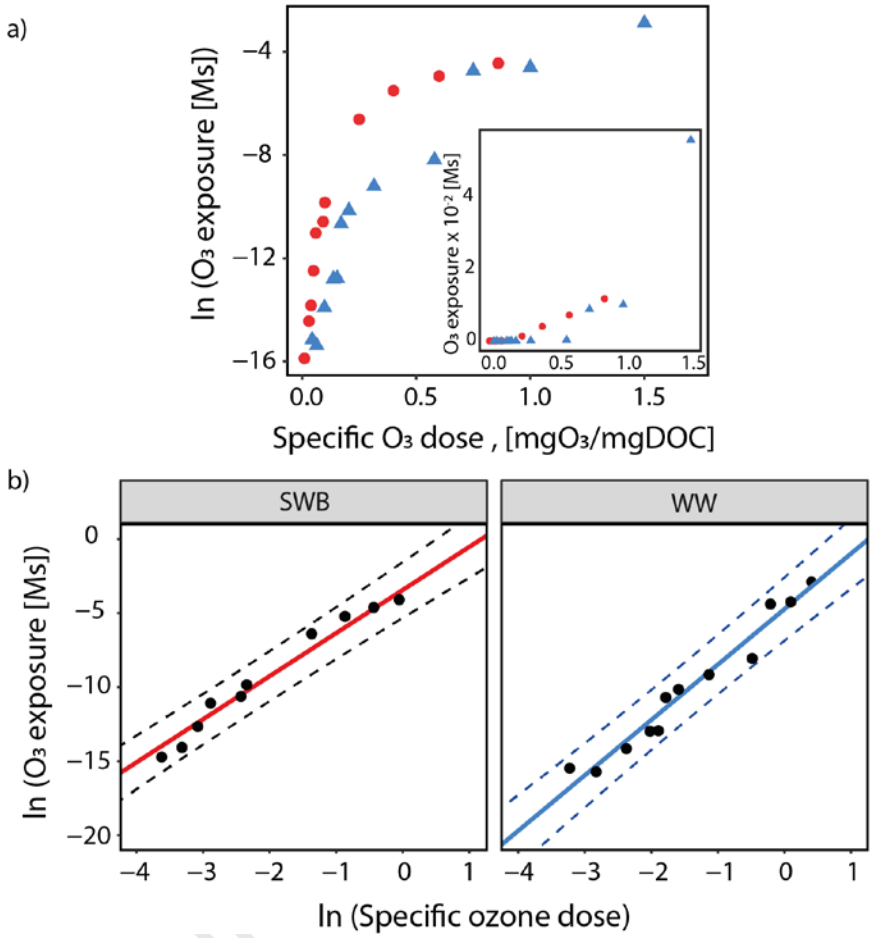


Figure 2. **Relationship between specific ozone dose and ozone exposure**. a) Natural logarithm of the measured $O_3$ exposure as a function of the ozone dose for SWB (red circles) and WW (blue triangles). The inset shows the $O_3$ exposure on a linear scale. b) Model fit according to equation 1 (solid lines) and 95% confidence intervals (dashed lines) on a logarithmic scale.

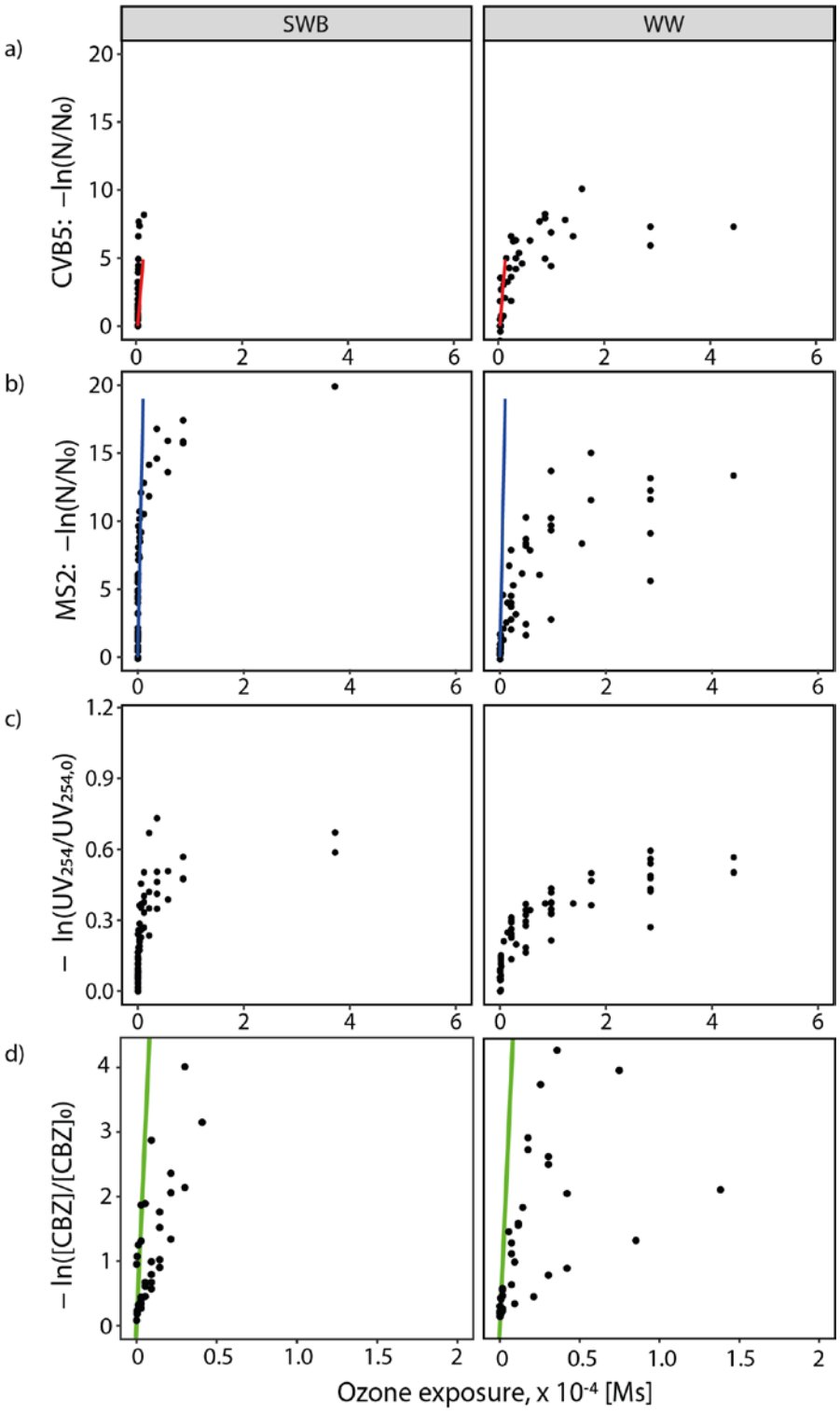


Figure 3. **Virus inactivation, $UV_{254}$ abatement and CBZ abatement as a function of the ozone exposure.** a) MS2 inactivation, b) CVB5 inactivation, c) $UV_{254}$ abatement, and d) CBZ abatement as a function of the ozone exposure for surface water of Lake Bret (SWB) and secondary effluent wastewater (WW). The colored lines show the corresponding inactivation and abatement estimated based on inactivation and second order inactivation rate constants determined previously (Wolf et al., 2018).

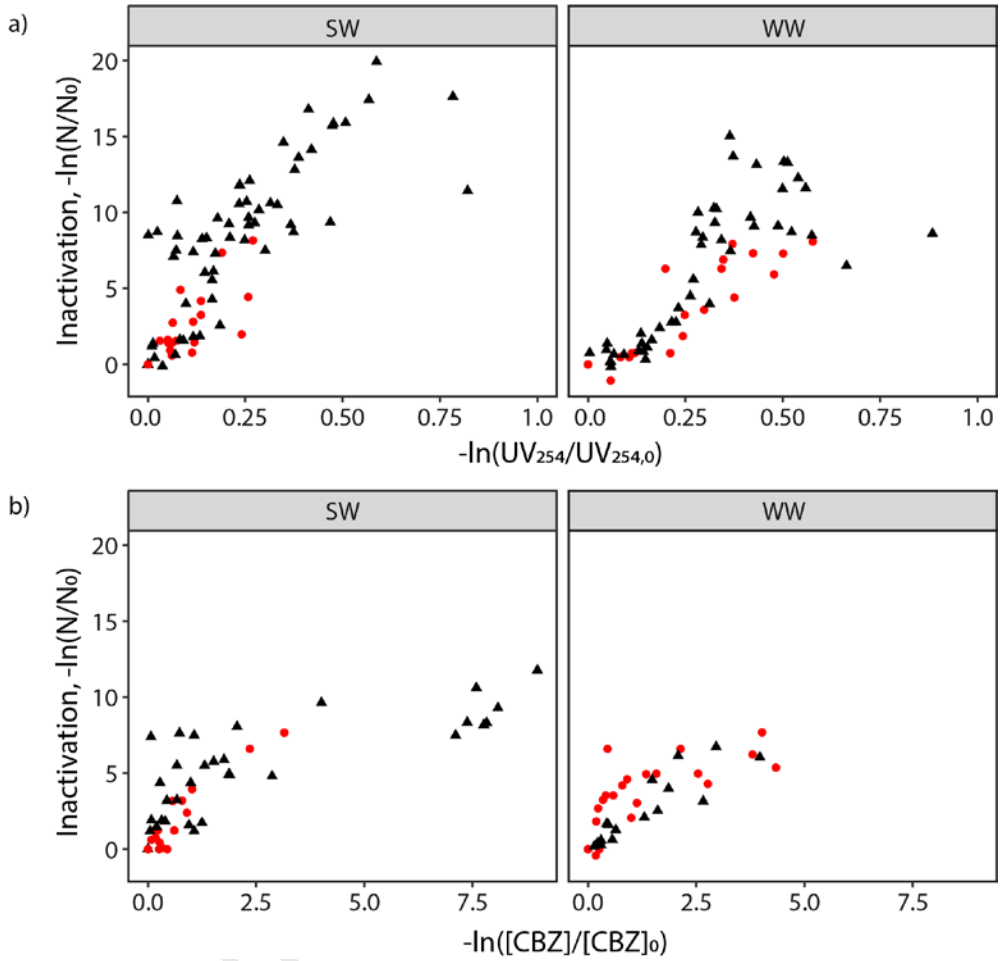


Figure 4. **Cross-correlations between virus inactivation and proxies.** ln-Inactivation of MS2 (black triangles) and CVB5 (red circles) as a function of a) the ln of the relative $UV_{254}$ abatement and b) the ln of the relative CBZ abatement.

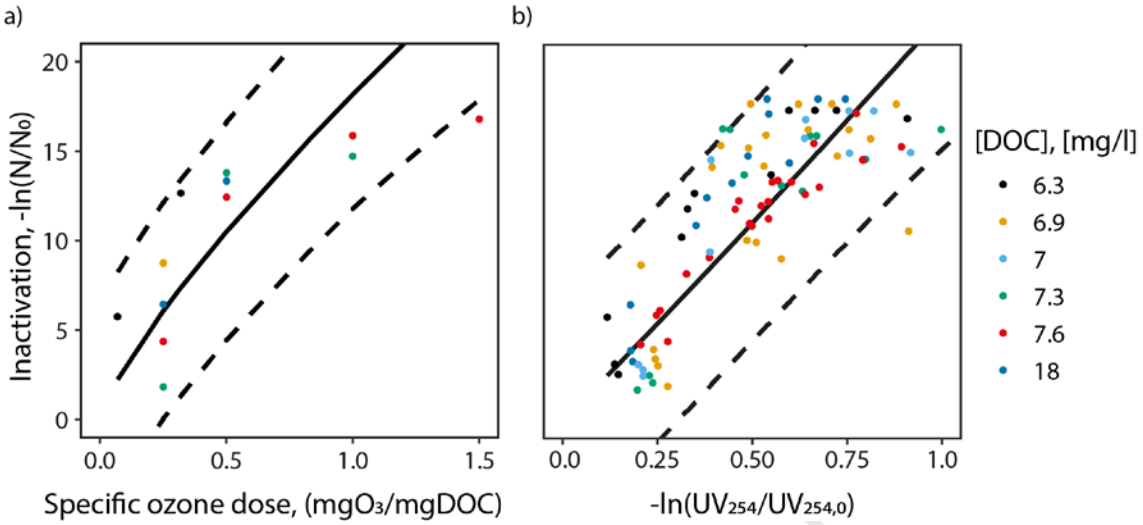


Figure 5. **Comparison of estimated virus inactivation with literature values**. Predicted MS2 inactivation (solid line) and 95% credible intervals (dashed line) as a function of a) specific ozone dose, and b) ln of the relative $UV_{254}$ abatement. Model predictions are compared with MS2 inactivation measured by a) *Gamage et al.* (2013) and b) *Gerrity et al.* (2012), who measured inactivation in wastewaters with different DOC contents (different colors).

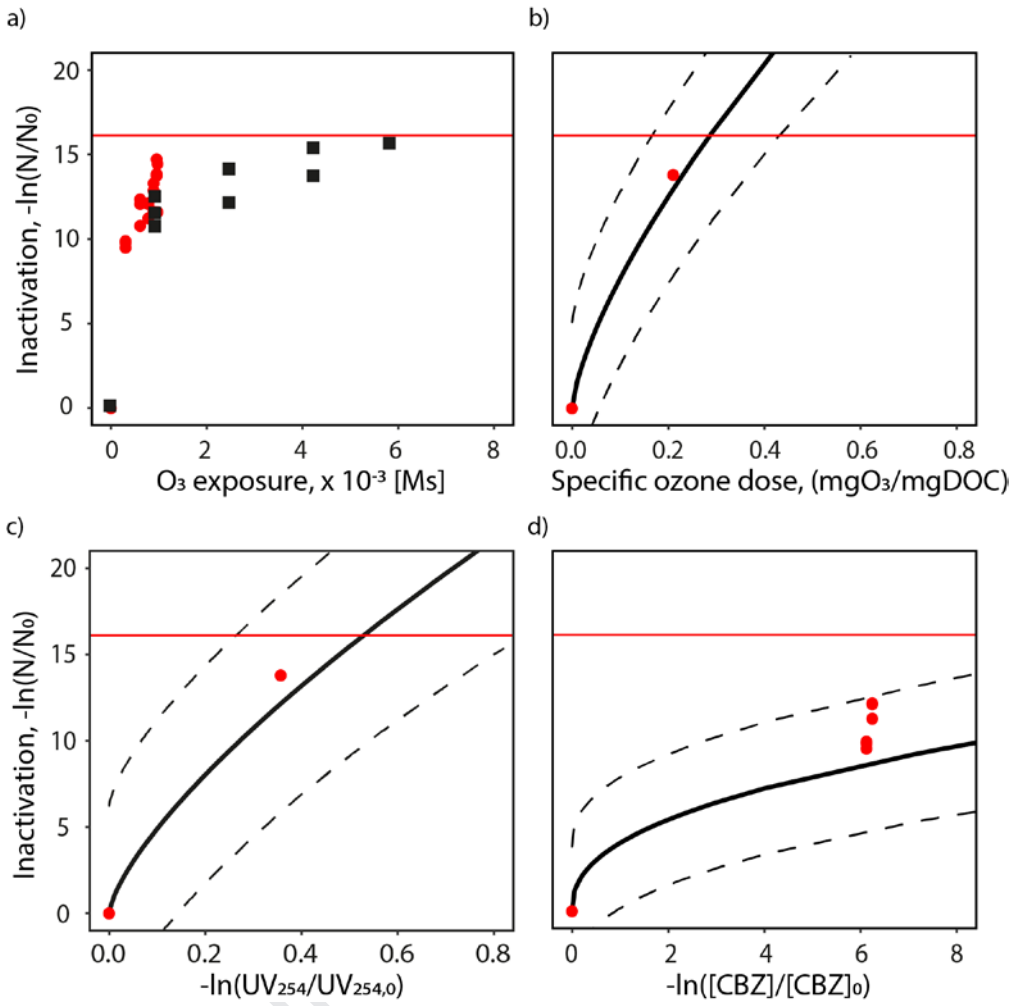


Figure 6. **Comparison of estimated and measured virus inactivation in a pilot-scale reactor.** MS2 inactivation was measured at two specific ozone doses: 0.2 $mgO_3$/mgDOC, which yielded measurable MS2 concentrations at all sampling points throughout the reactor (red circles); and 0.6 $mgO_3$/mgDOC, which resulted in measurable MS2 concentrations up to sampling point P3 (black squares). Inactivation as a function of a) the measured ozone exposure; b) the specific ozone dose; c) the ln of the relative $UV_{254}$ abatement; and d) the ln of the relative CBZ abatement. Data are compared with the mean inactivation (solid line) and 95% credible intervals (dashed lines) predicted based on equation 2. The red horizontal line represents the limit of quantification of MS2 inactivation.

Highlights

- Inactivation of two viruses by ozone was studied in surface water and lake water
- Inactivation coincided with the abatement of two proxies, $UV_{254}$ and carbamazepine
- Both proxies and the specific ozone dose can be used to estimate virus inactivation
- The application of the proxies was validated in a pilot-scale ozone reactor

**Declaration of interests**

☒ The authors declare that they have no known competing financial interests or personal relationships that could have appeared to influence the work reported in this paper.

☐The authors declare the following financial interests/personal relationships which may be considered as potential competing interests: